FINITE ELEMENT ANALYSIS OF SLIDING CONTACT BETWEEN A CIRCULAR ASPERITY AND AN ELASTIC URFACE IN PLANE STRAIN CONDITION

S. Subutay Akarca,
University of Windsor
401 Sunset Ave. Windsor, ON, CANADA N9B 3P4
Telephone: (519) 253 3000 ext.2605
Facsimile: (519) 973 7007

Dr. William J. Altenhof,
University of Windsor
401 Sunset Ave. Windsor, ON, CANADA N9B 3P4
Telephone: (519) 253 3000 ext.2619
Facsimile: (519) 973 7007

Dr. Ahmet T. Alpas,
University of Windsor
401 Sunset Ave. Windsor, ON, CANADA N9B 3P4
Telephone: (519) 253 3000 ext.2602
Facsimile: (519) 973 7007

Keywords: FEA, Sliding Wear, Surface Contact, Wear Simulation

ABSTRACT

Wear is a critical phenomenon affecting service life of products. Therefore, wear prediction is an important concern of study. In this study, sliding contact was modeled using LS-DYNA. FEMB was used to create the geometry of the model and the input file was manually modified as necessary. Studies were done to test, calibrate, and validate the model in LS-DYNA before simulation of the sliding wear by an asperity sliding over a plastically deforming and work hardening material surface.

A flat half-space with dimensions of 30μm depth and 100μm width is subjected to sliding contact by a semicircular asperity of radius 10μm. The third dimension of the model was assumed to be infinite and therefore a plane strain condition was studied. Elastic indentations were performed to validate the finite element model. Elastic indentation results were compared to the predictions of the Hertz theory of elastic contact. With the help of mesh convergence study the best conditions to simulate sliding wear were determined. Mesh dimensions, hourglass control, contact algorithm, application of the normal load, and mass scaling were the main issues of the study.

According to the Hertz theory, the maximum contact pressure and the maximum shear stress were calculated as 2684 and 805 MPa for the conditions studied. Numerical models predicted 10-15% higher values higher values for those stresses. However, normalized stress values show a very good agreement with the theoretical predictions.

INTRODUCTION

Sliding wear is a progressive or rapid loss of material from surfaces due to the relative motion between two bodies in contact under applied load[1,2]. Wear may cause catastrophic failure or reduce operating efficiency. Hence, wear is an active area of research.

Numerical analysis of sliding wear is a relatively new concern. Studies to simulate wear have begun in the late seventies and grown with the improvement of computer technology. Most of early-published finite element analysis models use materials with either elastic or elastic-perfectly plastic properties. With the help of advanced computers, more complex systems can be modeled. In the tribology field finite element analysis methods have been used to model rolling contact[3-5], spinning contact[6], and sliding contact[7-10].

Finite element techniques have been also applied to indentation research to simulate hardness tests[11-13], to define material properties[14-16], and to model crack growth[17]. In addition, elastic indentation is a very good method to verify the numerical model. The aim of this study is to create a credible and reliable finite element model that can be used to simulate sliding contact between two linear elastic surfaces. To achieve this purpose, different indentation models were tested and compared to the Hertz theory of elastic contact. Lu and Bogy[18] studied the effect of tip radius on nano-indentation hardness tests and verified their model by comparing elastic indentations to the Hertz theory of elastic indentation. In the same way, Sun et.al.[19] tested correctness of their model for deformation of various TiN coatings. By using the same approach, Podra and Andersson[8] verified their sliding wear simulations. In this study, the approach used to verify finite element models by previous investigators was improved and a better way of verification study was done.

FINITE ELEMENT MODEL

LS-DYNA version 960 was used to simulate sliding wear. FEMB was used to create the geometry of the model and the input file was manually modified as necessary.

Model Geometry

Surfaces of materials are not smooth. The surfaces have microscopic hills and valleys referred to as asperities. Hence, contact between two solids occurs at areas of individual points at the tip of asprities[2]. To model this, an asperity of cylindrical shape was assumed and defined to slide over a half-space.

A half-space of 30μm width and 100μm length was subjected to sliding contact by a semicircular asperity of radius 10μm. The half-space was assumed to have elastic properties of an A356 aluminum alloy. The third dimension of the half-space and the asperity were assumed as infinite and therefore a plane strain condition was created. Figure 1 shows the geometry of the model.

Since plane strain condition was studied, element formulation 13 was selected for the shell elements to simulate plane strain condition.

Application of Normal Load

The asperity was loaded with a total force of 3.3 N. To define the value of the load applied, different loads were considered and the depth of surface deformation was compared to actual indentation test results made at the same load using a nano-hardness indenter. When loads larger than 3.3 N were used, surface deformation depths were extensive and extended much larger than those experimentally observed. The normal load was applied in such a way that it was distributed equally on each node located on the top layer of the asperity. All nodes at the bottom layer of the half-space were constrained from motion.

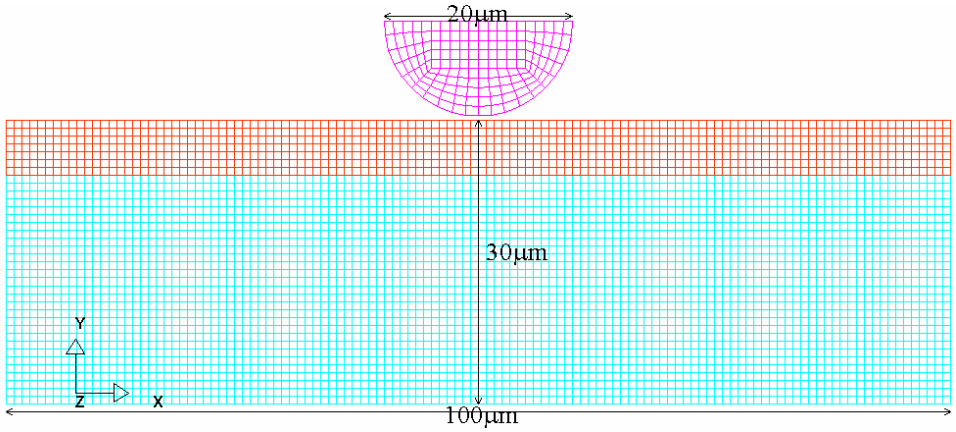

Figure 1. Geometric Details of the Model

The load application curve is presented in Figure 2. The load was ramped up from zero to a maximum value of 3.3 N in 0.0003 seconds and was then held constant for the remaining time (i.e. up to 0.001 seconds). Initially different ramping paths were studied (0.0005 seconds and 0.0002 seconds) and since there was no difference in deformation response of the surface, 0.0003 seconds ramping time was selected as the optimum duration for the load application.

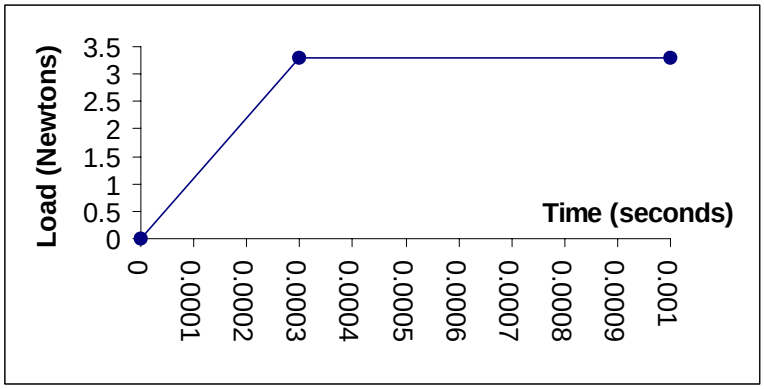

Figure 2. Load Curve

Material Properties

"Material type 1" (i.e., "MAT_ELASTIC" keyword) was used for the half-space. This is an isotropic elastic material and is available for shell elements in LS-DYNA[20]. Additionally the half-space was assumed to have Young's Modulus, Poisson's ratio, and mass density values equivalent those of an aluminum alloy (A356).

In the first attempt the asperity was modeled as a rigid material. In this case, "Material type 20" (i.e., "MAT_RIGID" keyword) was used to model the material properties of the asperity. However, the program did not start running because of small geometry, and inertia related problems occurred. As a second attempt, the asperity was modeled as a cylindrical rigidwall. Both "RIGIDWALL_GEOMETRIC_CYLINDER_MOTION" and "RIGID_WALL_GEOMETRIC_FLAT_MOTION" options were tried. In these simulation attempts, no contact between the asperity and the half-space occurred. Consequently, it was decided to model the asperity as an elastic material ("Material type 1"; "MAT_ELASTIC"). Of course, this material model has increased simulation time. Material properties of the asperity and the half-space are shown at Table1.

Table 1. Material Properties of the Half-Space and the Asperity

Part	Young's Modulus (GPa)	Poisson's Ratio	Mass Density (kg/m^3)	LS-DYNA Material Type
Half-Space	72.4	0.33	2669	1 (elastic)
Asperity	400.0	0.30	7800	1 (elastic)

Hourglass Control

In the preliminary runs, it was observed that hourglass control is needed for the model. Hence, hourglass control was applied both to upper portion of the half-space and to the asperity. Since hourglass control prolonged the simulation time, in order to save CPU time, hourglass control was applied only to a critical top layer of the half-space. Half-space was divided into two parts with same material properties; one with hourglass control and the other with the standard LS-DYNA default hourglass control. For non-default hourglass control, *HOURGLASS keyword was used with hourglass control type 4 and hourglass coefficient of value 0.05.

Mass Scaling

Usage of small sized mesh has caused long simulation times. To save time, mass scaling was applied. Test runs showed that mass scaling did not affect the results and can be used safely. This is shown in Table 2 that compares the results of two runs with exactly same inputs; one with mass scaling and the other without it.

Table 2. Examination of Mass Scaling Results

Energy (J), Stress (Pa)	Run1(without mass scaling)	Run1(with 23.8 times mass scaling)
Max. Internal Energy	1.83947×10^{-6}	1.83869×10^{-6}
Kinetic Energy	0.680564×10^{-8}	0.797265×10^{-8}
Hourglass Energy	0.921898×10^{-8}	1.02855×10^{-8}
Sliding Interface Energy	0.2052694×10^{-7}	0.2785055×10^{-7}
Max. Shear Stress	4.151×10^{8}	4.151×10^{8}
Max. Hydrostatic Stress	5.596×10^{8}	5.597×10^{8}
First Principal Stress	-4.203×10^{8}	-4.202×10^{8}
Second Principal Stress	-5.586×10^{8}	-5.586×10^{8}
Third Principal Stress	-8.084×10^{8}	-8.082×10^{8}

Contact Algorithm

The contact algorithm "CONTACT_2D_AUTOMATIC_NODE_TO_SURFACE" was used for simulating contact between the asperity and the half-space. It defines a 2-dimensional contact and can be used with shell elements using plane strain formulations[20]. Static and dynamic coefficients of friction were set to zero to study frictionless condition. First, scale factor for the penalty force stiffness was defined as default value of 1. Due to excessive penetrations the default value of the penalty scale factor was increased by 8 times to maintain a low level of penetration.

Mesh Convergence

Three different meshes were created and examined to investigate mesh convergence. These three models have the same geometry and properties, except for element sizes. Table 3 compares all four different models examined. Model C and Model D are the same models with different mass scaling. Figures 3 to 5 illustrates a portion of all the models.

Table 3. Comparison of Different Meshed Elastic Indentation Models

Model	Min. Element Size (μm)	Total Number of Elements	Total Number of Nodes	Mass Scaling (Times)	Aspect Ratio
Model A	0.8333	4470	4648	40.6	2.7
Model B	0.4167	8952	9186	18.1	2.7
Model C	0.2083	7864	8128	6.04	2.7
Model D	0.2083	7864	8128	3.6	2.7

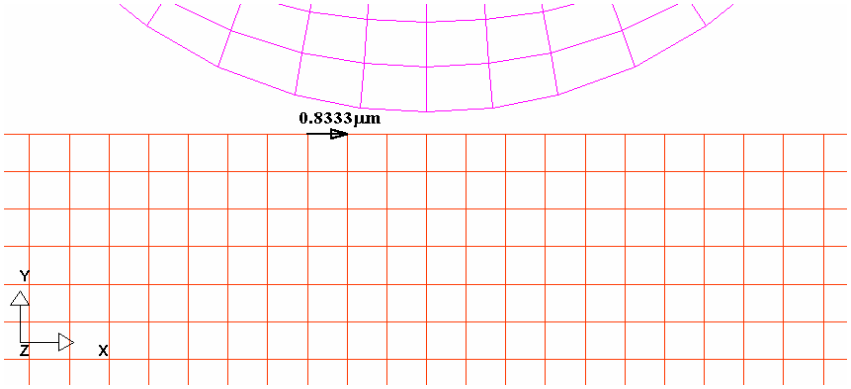

Figure 3. Model A (Minimum Element Size: 0.8333µm

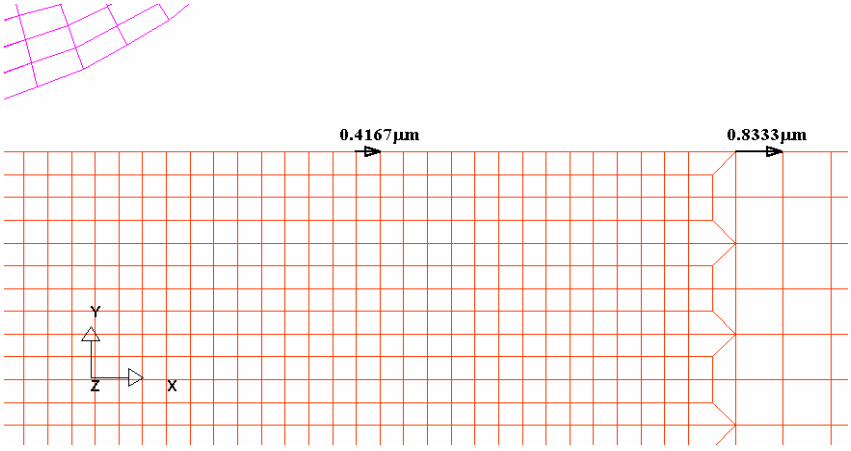

Figure 4. Model B (Minimum Element Size: 0.4167µm)

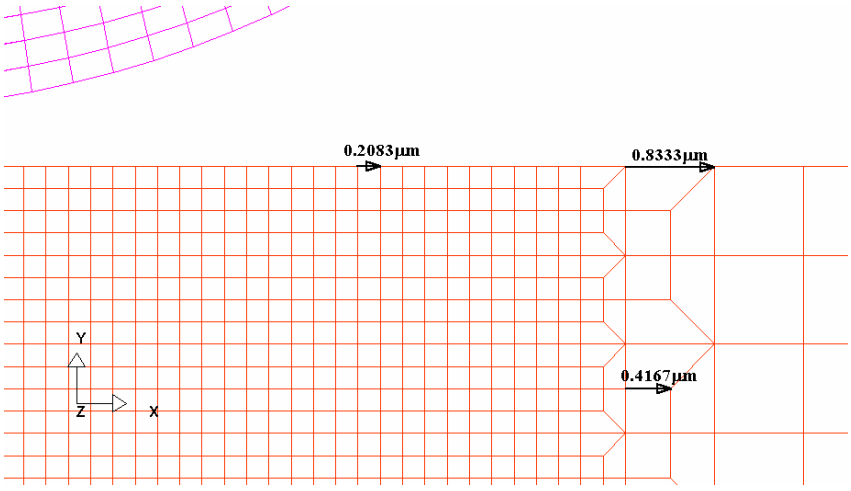

Figure 5. Model C and Model D (Minimum Element Size: 0.2083µm)

VERIFICATION OF THE FINITE ELEMENT MODEL

Since the aim of this study is to assess the validity of the finite element model, the results of the elastic indentations performed between the asperity and the half-space were compared with those obtained from the Hertz theory of elastic contact.

Hertz has formulated the stresses at the contact of two elastic solids. He has made the hypothesis that in general when two cylinders are pressed each other or when a cylinder is loaded against a half-space, the area of contact is elliptical in shape (Figure 6 and 7.). He has formulated this elliptical pressure distribution. The pressure at any position x is given by[21]:

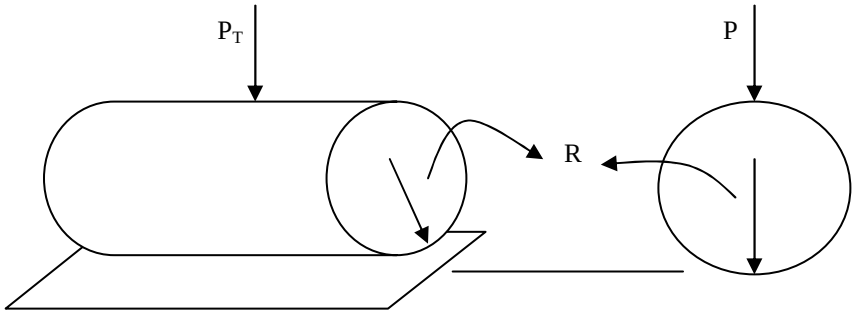

Figure 6. Contact between the Asperity and the Half-space (P_T: Total Force Applied, P: Force per Unit Length, R: Radius)

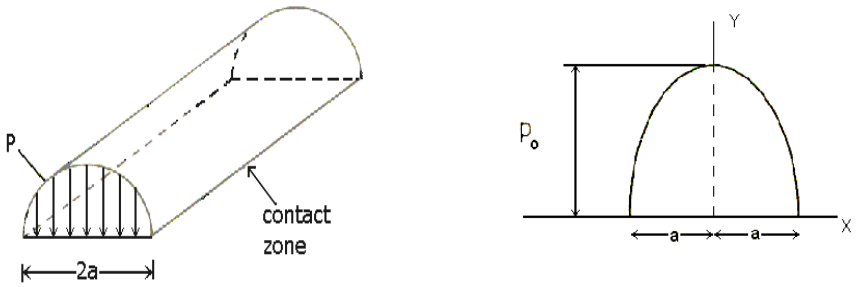

(a) (b)

Figure 7. (a) Area of Contact in Hertz Theory, (b) Maximum Contact Pressure and Axes

$$p = p_O(1-(x/a)^2)^{1/2} \quad (1)$$

where; p: pressure distribution,
p_O: maximum contact pressure.

The equation relating applied load (P) to the maximum contact pressure (p_O) within solids is as follows[21]:

$$P_0 = \sqrt{\frac{PE^*}{\pi R}} \quad (2)$$

The semi-contact length (a) is given as:

$$a = \sqrt{\frac{4PR}{\pi E^*}} \tag{3}$$

where;

$$E^* = \left(\frac{1-\nu_1{}^2}{E_1} + \frac{1-\nu_2{}^2}{E_2} \right)^{-1} \tag{4}$$

In this work
ν_1=0.33, E_1=72.4GPa;
ν_2=0.30, E_2=400GPa;
R: radius of asperity = 10μm
P: applied normal load per unit length = 3300 kgmm/s^{2}mm=3300kg/s^2

Johnson[21] gives Hertz's formulations for stresses in solids along y axis at x=0 as:

$$\sigma_X = -\frac{p_O}{a}\left\{(a^2+2y^2)(a^2+y^2)^{-1/2} - 2y\right\} \tag{5}$$

$$\sigma_y = -p_O a (a^2+y^2)^{-1/2} \tag{6}$$

$$\sigma_Z = \nu(\sigma_X + \sigma_Y) \tag{7}$$

$$\tau = -\frac{p_O}{a}\left\{y - y^2(a^2+y^2)^{-1/2}\right\} \tag{8}$$

The theory predicts maximum shear stress value as $\tau = 0.30p_0$ at x=0, y=0.78a.

To verify finite element model, results of the equation 1 and equations 5-8 were used and compared to the results of the numerical model.

DISCUSSION OF RESULTS

Table 4 presents predictions of the Hertz theory with the results of simulations conducted in this research. Except for Model A, predictions of models are very close to each other. Model A predicts the critical depth for maximum shear stress incorrectly, due to its large mesh size and hence it is discarded. The other models (B-D) predict 10-15% higher values of stress than those predicted by the Hertz theory. However, their contact width and maximum shear stress position predictions are very similar to that of Hertz theory. Figure 8 shows the position of maximum shear stress for Model D.

Table 4. Comparison of Elastic Indentation Model Results and Hertz Theory Calculations

MODEL	P_0 (MPa)	Max. Shear Stress (MPa)	y (at τ_{max}) (μm)	a (μm)	y/a
Hertz Theory	2683.85	805.155	0.611	0.783	0.78
Model A	2105.73	631.718	0.8333-1.6666	0.8333-1.6666	0.5-1
Model B	3122.37	936.712	0.4167-0.8333	0.8333-1.2501	0.33-1
Model C	3121.30	936.39	0.6249-0.8333	0.8333-1.0415	0.6-1
Model D	3000.87	900.263	0.6249-0.8333	0.8333-1.0415	0.6-1

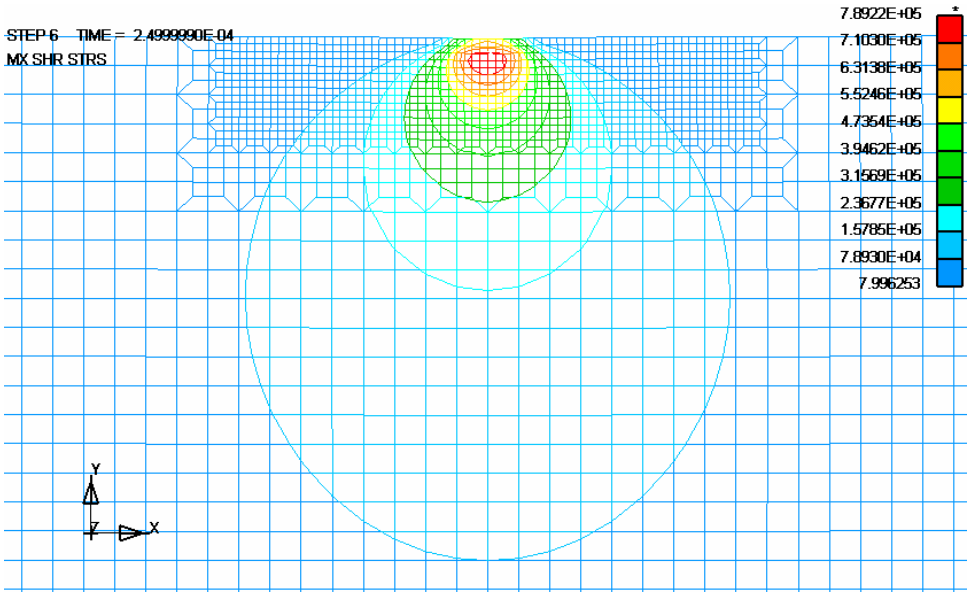

Figure 8. Position of Maximum Shear Stress after Indentation

Some investigators tested their models by using equation 1[8,18,19]. In the following figure, the same approach was used to examine the pressure distribution predictions of models by comparing to Hertz's elliptical shape contact area theory. Numerical models of a cylindrical asperity loaded against a half-space showed that the area of contact had approximately an elliptical shape. It can be seen that a very good agreement achieved especially among Model C, Model D and the theoretical solution.

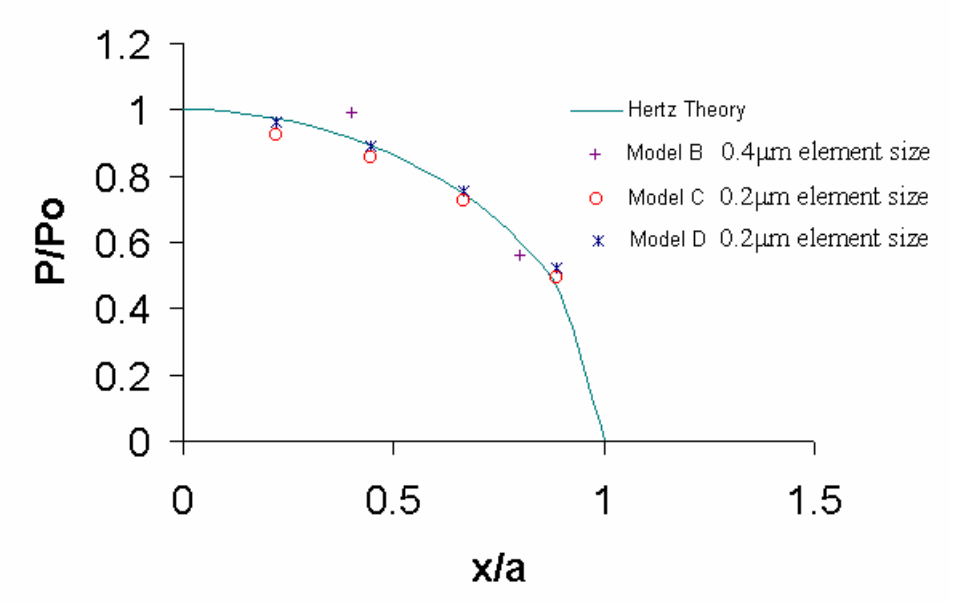

Figure 9. Comparison of Pressure Distribution in Contact Zone Obtained by the Finite Element Models and the Analytical Solutions

A better way of examining the validity of the results can be achieved by plotting the variations of σ_X, σ_Y and τ with depth below the surface using equations 5-8. When equation 1 is used, it only tests pressure distribution in contact zone. However, with the new approach, numerical models can be verified by examining the variations of stress distributions in the half-space material. Figure 10 shows such a plot for the predictions of the Hertz theory and the numerical models of this work. From the figure it can be said that Model B shows a higher deviation from the theory. Both models for 0.2 μm element size (Models C and D) agree well with the theoretical solutions and can be used for sliding wear simulations appropriately.

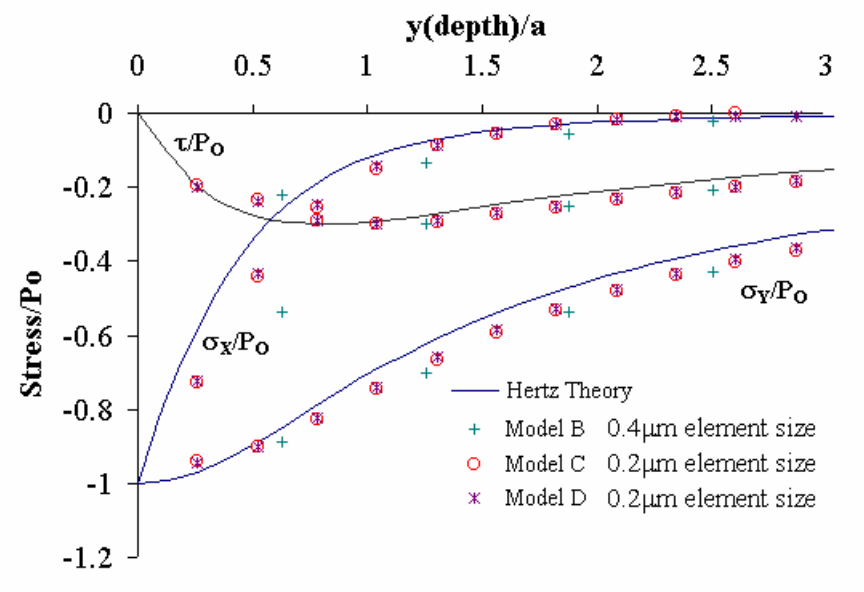

Figure 10. Comparison of Subsurface Stresses along Axis of Symmetry

As a result of verification studies, Model D was chosen in order to use in the sliding wear simulations because it contains less mass scaling compared with the Model C and produced the closest agreement with the Hertz model.

It should be noted that the maximum shear stress values obtained from the finite element (and the analytical) solutions exceed the yield strength of A356 aluminum alloy (165MPa). A regression analysis showed that the stress-strain relation for the material layers adjacent to the contact surfaces of aluminium alloys could be represented using Voce type equation and this equation will be used for the future sliding wear simulations.

CONCLUSIONS

1- Indentation of a circular asperity to an elastic surface in plane strain condition was studied to verify the applicability of finite element models to simulate sliding wear contact.

2- Comparison of the finite element analysis results with those of the Hertz theory of elastic contact has proved that sliding wear can be modeled accurately using LS-DYNA finite element analysis program.

3- To verify simulation results, pressure distribution predictions of the models were compared with those of the Hertz theory. In addition, numerical models were tested by assessing the distribution of stresses below the contact surfaces. This is a new and a better approach to validate simulation results.

4- A mesh convergence study was used to determine the most appropriate model for simulation of sliding wear. For the problem studied, the Hertz theory predicts a maximum contact pressure of 2684 MPa and a contact width of 0.78μm. Model D (with 0.2μm element size) predicts a maximum contact pressure of 3000 MPa and a contact with of 0.9μm. Thus, Model D is found to be the most suitable one among the models examined

5- The results indicated that stress levels produced in the workpiece material under applied load condition is much higher than the yield strength of the half-space material. Therefore, results showed the need for elastic-plastic analysis.

REFERENCES

1- Friction and Wear Testing Source Book of Selected References from ASTM Standards and ASM Handbooks, ASM International, Materials Park, OH., 1997, pp.101.
2- Zum Gahr K.H., "Microstructure and Wear of Materials", Elsevier, New York, 1987, pp. 4, 48, and 351.
3- Bhargava V., Hahn G.T., and Rubin C.A., "An Elastic-Plastic Finite Element Model of Rolling Contact, Part1: Analysis of Single Contacts", Transactions of ASME, 1985, Vol.52, pp.67-74.
4- Bhargava V., Hahn G.T., and Rubin C.A., "An Elastic-Plastic Finite Element Model of Rolling Contact, Part2: Analysis of Repeated Contacts", Transactions of ASME, 1985, Vol.52, pp.75-82.
5- Franklin F.J., Widiyarta I., and Kapoor A., "Computer Simulation of Wear and Rolling Contact Fatigue", Wear, 2001, Vol.251, pp.949-955.
6- Podra P., and Andersson S., "Finite Element Analysis Wear Simulation of a Conical Spinning Contact Considering Surface Topography", Wear, 1999, Vol.224, pp.13-21.
7- Ohmae N., and Tsukizoe T., "Analysis of a Wear Process Using the Finite Element Method", Wear, 1980, Vol.61, pp.333-339.
8- Podra P., and Andersson S., "Simulating Sliding Wear with Finite Element Method", Tribology International, 1999, Vol.32, pp.71-81.
9- Molinari J.F., Ortiz M., Radovitzky R., and Repetto E.A., "Finite Element Modeling of Dry Sliding Wear in Metals", Engineering Computations, 2001, Vol.18, No.3/4, pp.592-609.
10- Ko P.L., Iyer S.S., Vaughan H., and Gadala M., "Finite Element Modeling of Crack Growth and Wear Particle Formation in Sliding Contact", Wear, 2001, Vol.251, pp.1265-1278.
11- Shu J.Y., and Fleck N.A., "The Prediction of a Size Effect in Micro-Indentation", Int. J. Solids Structures, 1998, Vol.35, No.13, pp.1363-1383.
12- Lichinchi M., Lenardi C., Haupt J., and Vitali R., "Simulation of Berkovich Nano-indentation Experiments on Thin Films Using Finite Element Method", Thin Solid Films, 1998, Vol.333, pp.278-286.
13- Yamamoto T., Kurishita H., and Matsui H., "Modeling of the Cyclic Ball Indentation Test for Small Specimens Using the Finite Element Method", Journal of Nuclear Materials, 1999, Vol.271&272, pp.440-444.
14- Zhang M., Zheng Y.P., and Mak A.F.T., "Estimating the Effective Young's Modulus of Soft Tissues from Indentation Tests", Med. Eng. Phys., 1997, Vol.19, No.6, pp.512-517.
15- Taljat B., Zacharia T., and Kosel F., "New Analytical Procedure to Determine Stress-Strain Curve from Spherical Indentation Data", Int. J. Solids Structures, 1998, Vol.35, No.33, pp.4411-4426.
16- Li W., Rodgers B., and et.al, "A Finite Element and Experimental Study of Punch and Bulge Testing", Key Engineering Materials, 1999, Vol.167&168, pp.55-63.
17- Zhang W., and Subhash G., " An Elastic-Plastic Cracking Model for Finite Element Analysis of Indentation Cracking in Brittle Materials", Int. J. Solids Structures, 2001, Vol.38, pp.5893-5913.
18- Lu C., and Bogy D.B., "The Effect of Tip Radius on Nano-Indentation Hardness Tests", Int. J. Solids Structures, 1995, Vol.32, pp.1759-1770.
19- Sun Y., Bloyce A., and Bell T., "Finite Element Analysis of Plastic Deformation of Various TiN Coating / Substrate Systems Under Normal Contact with a Rigid Sphere", Thin Solid Films, 1995, Vol.271, pp.122-131.
20- LS-DYNA 960 User's Manual, Livermore Software Technology Corporation, March 2001.
21- Johnson K.L., "Contact Mechanics", Cambridge University Press, New York, 1985.